Color effects from scattering on random surface structures in dielectrics.

Clausen, Jeppe; Christiansen, Alexander B; Garnæs, Jørgen; Mortensen, N. Asger; Kristensen, Anders

Published in:
Optics Express

Link to article, DOI:
10.1364/OE.20.004376

Publication date:
2012

Document Version
Publisher's PDF, also known as Version of record

Color effects from scattering on random surface structures in dielectrics

Jeppe Clausen,[1,4] **Alexander B. Christiansen,**[2,4] **Joergen Garnaes,**[3] **N. Asger Mortensen,**[1] **and Anders Kristensen**[2]

[1]*Department of Photonics Engineering, Technical University of Denmark, Oersteds Plads, Building 343, DK-2800 Kgs. Lyngby, Denmark*
[2]*Department of Micro and Nanotechnology, Technical University of Denmark, Oersteds Plads, Building 345B, DK-2800 Kgs. Lyngby, Denmark*
[3]*Danish Fundamental Metrology, Matematiktorvet, Building 307, DK-2800 Kgs. Lyngby, Denmark*
[4]*Both authors have contributed equally.*

*anders.kristensen@nanotech.dtu.dk

Abstract: We show that cheap large area color filters, based on surface scattering, can be fabricated in dielectric materials by replication of random structures in silicon. The specular transmittance of three different types of structures, corresponding to three different colors, have been characterized. The angle resolved scattering has been measured and compared to predictions based on the measured surface topography and by the use of non-paraxial scalar diffraction theory. From this it is shown that the color of the transmitted light can be predicted from the topography of the randomly textured surfaces.

OCIS codes: (050.1940) Diffraction; (220.4241) Nanostructure fabrication; (330.1690) Color; (290.0290) Scattering.

References and links

1. C. G. Bernhard, "Structural and functional adaptation in a visual system," Endeavour **26**, 79–84 (1967).
2. P. B. Clapham and M. C. Hutley, "Reduction of lens reflexion by the moth eye principle," Nature **244**, 281–282 (1973).
3. S. Kinoshita, S. Yoshioka, and J. Miyazaki, "Physics of structural colors," Rep. Prog. Phys. **71**, 076401 (2008).
4. Y. Yoon, H. Lee, S. Lee, S. Kim, J. Park, and K. Lee, "Color filter incorporating a subwavelength patterned grating in poly silicon," Opt. Express **16**, 2374–2380 (2008).
5. H. Lee, Y. Yoon, S. Lee, S. Kim, and K. Lee, "Color filter based on a subwavelength patterned metal grating," Opt. Express **15**, 15457–15463 (2007).
6. Y. Kanamori, M. Shimono, and K. Hane, "Fabrication of transmission color filters using silicon subwavelength gratings on quartz substrates," IEEE Photon. Technol. Lett. **18**, 2126–2128 (2006).
7. Y. Ye, Y. Zhou, H. Zhang, and L. Chen, "Polarizing color filter based on a subwavelength metal-dielectric grating," Appl. Opt. **50**, 1356–1363 (2011).
8. C. Genet and T. W. Ebbesen, "Light in tiny holes," Nature **445**, 39–46 (2007).
9. X. Hu, L. Zhan, and Y. Xia, "Color filters based on enhanced optical transmission of subwavelength-structured metallic film for multicolor organic light-emitting diode display," Appl. Opt. **47**, 4275–4279 (2008).
10. R. Leitel, A. Kaless, U. Schulz, and N. Kaiser, "Broadband antireflective structures on pmma by plasma treatment," Plasma Process. Polym. **4**, S878–S881 (2007).
11. I. Wendling, P. Munzert, U. Schulz, N. Kaiser, and A. Tünnermann, "Creating anti-reflective nanostructures on polymers by initial layer deposition before plasma etching," Plasma Process. Polym. **6**, S716–S721 (2009).
12. C. Ting, M. Huang, H. Tsai, C. Chou, and C. Fu, "Low cost fabrication of the large-area anti-reflection films from polymer by nanoimprint/hot-embossing technology," Nanotechnology **19**, 205301 (2008).
13. H. Schift and A. Kristensen, "Nanoimprint lithography—patterning of resists using molding," in *Springer Handbook of Nanotechnology,* B. Bhushan, ed. (Springer, 2010), pp. 271–312.

#161219 - $15.00 USD Received 10 Jan 2012; revised 2 Feb 2012; accepted 2 Feb 2012; published 7 Feb 2012

14. L. Sainiemi, V. Jokinen, A. Shah, M. Shpak, S. Aura, P. Suvanto, and S. Franssila, "Nonreflecting silicon and polymer surfaces by plasma etching and replication," Adv. Mater. **23**, 122–126 (2011).
15. H. Jansen, M. d. Boer, R. Legtenberg, and M. Elwenspoek, "The black silicon method: a universal method for determining the parameter setting of a fluorine-based reactive ion etcher in deep silicon trench etching with profile control," J. Micromech. Microeng. **5**, 115–120 (1995).
16. S. Aura, V. Jokinen, L. Sainiemi, M. Baumann, and S. Franssila, "UV-embossed inorganic-organic hybrid nanopillars for bioapplications," J. Nanosci. Nanotechno. **9**, 6710–6715 (2009).
17. D. Domine, F. J. Haug, C. Battaglia, and C. Ballif, "Modeling of light scattering from micro- and nanotextured surfaces," J. Appl. Phys. **107**, 044504 (2010).
18. J. E. Harvey, "Fourier treatment of near-field scalar diffraction theory," Am. J. Phys. **47**, 974 (1979).
19. J. E. Harvey, C. L. Vernold, A. Krywonos, and P. L. Thompson, "Diffracted radiance: a fundamental quantity in nonparaxial scalar diffraction theory," Appl. Opt. **38**, 6469–6481 (1999).

1. Introduction

Nature has demonstrated optical effects such as antireflection and colors based on micro and nanostructures. Well known examples are anti reflective moth eye structures [1,2] and iridescent butterfly wings [3]. This has stimulated biomimetic research on obtaining such functionality by micro and nanofabrication methods. Optical effects that rely solely on surface topography has the potential for cost-efficient manufacturing in cheap polymers by embossing/imprinting or injection molding and can provide an alternative for chemical additives or multilayer deposition requiring vacuum methods.

This paper addresses structural color filters. Such devices have been proposed that are based on either sub-wavelength one dimensional gratings [4–7] or nano-holes in metal surfaces that rely on plasmon enhanced propagation [8, 9]. These filters are all multi-material devices, and require several process steps to fabricate.

The results in this paper show that structural color filters can be produced in a single material, without use of pigments, dyes or multi-material sub wavelength structures. We demonstrate the application of strong scattering on random surface structures with dimensions close to the wavelength of the light. The structures show color effects in the direct transmission of white light, when fabricated in an otherwise fully transparent and colorless material and the textured surfaces thereby work as structural color filters fabricated in a single material. The optical performance of the demonstrated color filters rely on mechanisms different from those of periodic color filters [4–9], which in general have higher efficiencies and smaller spectral widths. On the other hand, the type of filter proposed here will benefit from a much lower fabrication cost.

The fabricated surfaces are characterized optically in transmission measurements and angle resolved scattering measurements. The measured results are compared to results calculated using diffraction theory and topographical information achieved by atomic force microscopy (AFM) and it is shown that for the investigated surface the specular transmittance can be predicted from an AFM-scan.

In recent years several methods for fabricating optically functional structures in polymeric materials have been investigated. For antireflective structures and structural color filters in polymers, the applications typically require large areas, making electron beam lithography inconvenient. Instead, methods like maskless plasma etching have been investigated which can fabricate randomly ordered nanostructures on large areas. The structures can be defined directly in the polymer surfaces e.g. by direct etching with a low pressure plasma [10] or by the use of an initial layer as random masking in a plasma etch [11].

Another approach is to fabricate the structures in a master and subsequently replicate them to the polymer. The replication process can be done by the use of an electroplated mold followed by hot embossing [12] or by casting a soft elastomeric mold from the master and subsequently use it for hot embossing or UV-nano imprint lithograpy (UV-NIL) [13, 14].

#161219 - $15.00 USD Received 10 Jan 2012; revised 2 Feb 2012; accepted 2 Feb 2012; published 7 Feb 2012

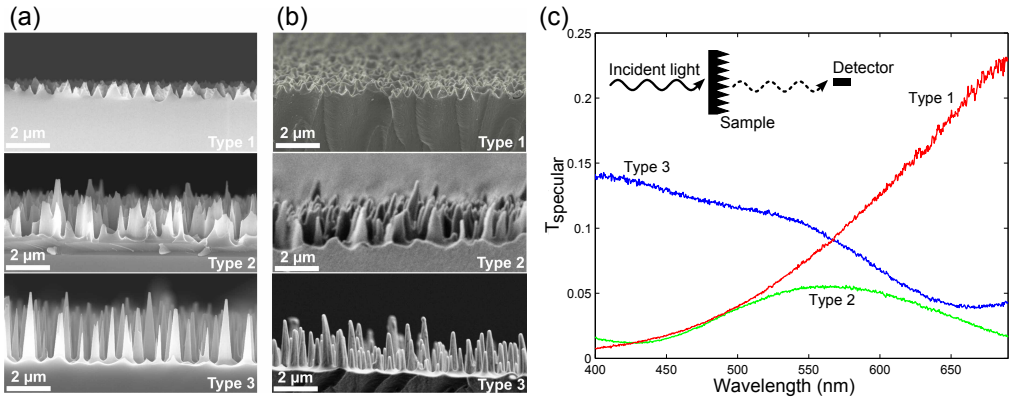

Fig. 1. (a) Three different types of random surface structures fabricated in silicon by reactive ion etching. (b) The corresponding replica in Ormocomp fabricated in an UV-NIL process using a PDMS stamp casted from the silicon surface. The sharp corners of the silicon structures are rounded in the replication process. (c) Transmittance spectra of the three types of Ormocomp surface structures. The spectra are measured normal to the surface for normal incident light. The three types of surfaces appear orange, green, and blue respectively, when seen against a white light source.

2. Experimental section

The random structures were fabricated in silicon using reactive ion etching (RIE-STS Cluster System C004) with a gas mixture of SF_6 (15 sccm) and O_2 (22.5 sccm). The pressure was 300 mTorr, the platen power was 200 W, and the etching time was 10 minutes. The structures appear due to micro masking and the formation of a SiO_xF_y layer, which passivates the silicon surface. The resulting type of structure is determined by the rate of which the passivation is formed and subsequently removed by flourine radicals [15]. Three different types of structures were seen on one wafer. The variations are due to non-uniformities of the etch in the radial direction of the wafer. The three different types of structures are seen in Fig. 1(a). In the center of the wafer the structures are of type 1, at a distance of 10 mm from the edge the structures are of type 2, and 4 mm from the edge the structures are of type 3. All structures have lateral sizes similar to the wavelength of visible light and are therefore not characterized as sub-wavelength structures. As shall be demonstrated this results in scattering of incoming light, and the variations in height, shape, and pitch of the different types of structures lead to different scattering characteristics when replicated in transparent materials.

The structures are replicated in the organic-inorganic hybrid polymer Ormocomp (Micro resist technology Gmbh, Berlin) based on the method described by Sainiemi *et al.* [14], where an elastomeric stamp is casted from the silicon and used in UV-NIL. The PDMS (Sylgard 184, Dow Corning) was mixed as recommended by the manufacturer and poured onto the master and left for degassing in a desiccator for 30 minutes prior to curing (65 degrees Celsius for 3 hours). The silicon master was coated with FDTS for anti adhesion.

Ormocomp was spin coated on a glass substrate to a thickness of approximately 50 µm. The imprints were performed in an Obducat NIL Imprinter 2.5 at room temperature with a hydrostatic pressure on the backside of the PDMS stamp (10 bar) for 10 minutes. The Ormocomp was cured with a UV-light source (1000 W for 10 minutes) through the glass substrate and the stamp was subsequently removed. The resulting replica of the silicon master are seen in Fig. 1(b). As expected from earlier reports the replicated structures are rounded [14, 16], but the main characteristics of the various structures are maintained in the replica.

#161219 - $15.00 USD Received 10 Jan 2012; revised 2 Feb 2012; accepted 2 Feb 2012; published 7 Feb 2012

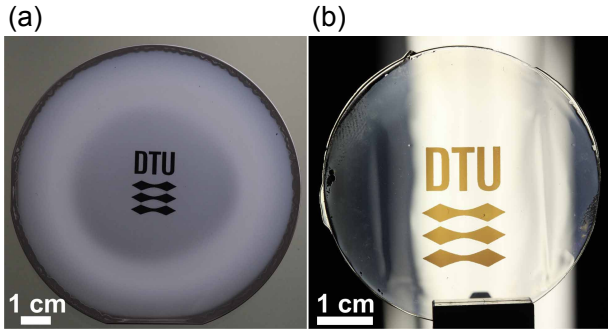

Fig. 2. (a) Silicon master with a black DTU-logo fabricated by selective removal of the surface structures around the logo using photolithography and isotropic silicon etching. The structures in the logo are of type 1 (Fig. 1(a)). (b) Replication in an Ormocomp film on a glass substrate fabricated by UV-NIL with a PDMS stamp casted from the master. When seen against a white light source the logo appears orange.

By using UV lithography the structures can be fabricated in specific patterned areas to make color filters of any macroscopic design. An example is seen in Fig. 2(a), where the pattern is seen as a black logo in the center of the silicon master. The structures in the logo are of type 1 and the corresponding replication is seen in Fig. 2(b). Here, the macroscopic logo is comprising wavelength scale structures not visible to the naked eye, yet causing the logo to appear orange when seen against the white light illumination.

All optical measurements were performed using a homebuild setup. The samples were illuminated at normal incidence with white light (Xenon lamp, HPX-2000). The light was collected in a fiber (500 μm in diameter) and analyzed in a spectrometer (Jaz, Ocean Optics). The setup made it possible to move the detecting fiber to any desired angle with respect to the sample.

AFM-images were scans of 20×20 μm^2 with a resolution of 512×512 pixels. The size of the scanned area influences the resolution of the scattering angle in the calculations [17] and is chosen such that good angular resolution is achieved while maintaining a sufficient spatial resolution in the AFM scan. The tip used was a high aspect ratio tip (Improved Super Cone type 125C40-R). Specifications according to the manufacturer: Tip height $>$ 7 μm, radius $<$ 10 nm, and full cone angle $<$ 10 degrees. The AFM used was a Metrology AFM based on a Dimension 3100 from Digital Instruments, Veeco Metrology Group (now Bruker) and a metrology head based on piezoelectric flexures equipped with capacitive distance sensors. All measurements were carried out in dynamic resonant mode.

3. Results and discussion

The structures have been characterized in the visible range from 400-700 nm. The specular transmission of light of the three types of structures is shown in Fig. 1(c). The quite different geometry of the three types also results in very different transmission spectra. The transmission spectrum of structures of type 1 shows much higher specular transmission for long wavelengths than for short wavelengths. The reason for this is wavelength dependent scattering which occurs at the structured surface, where light with short wavelength is scattered more than light with long wavelength. The opposite is the case for the transmission spectrum of type 3, where red light is scattered more than blue light. For type 2 a peak in the transmission at 560 nm is observed. The three different transmission spectra illustrate the color appearance of the different areas of the imprint when seen against white light. Type 1 appears orange, type 2 appears green, and type 3 appears blue. In order to investigate the scattering behavior in more detail,

#161219 - $15.00 USD Received 10 Jan 2012; revised 2 Feb 2012; accepted 2 Feb 2012; published 7 Feb 2012

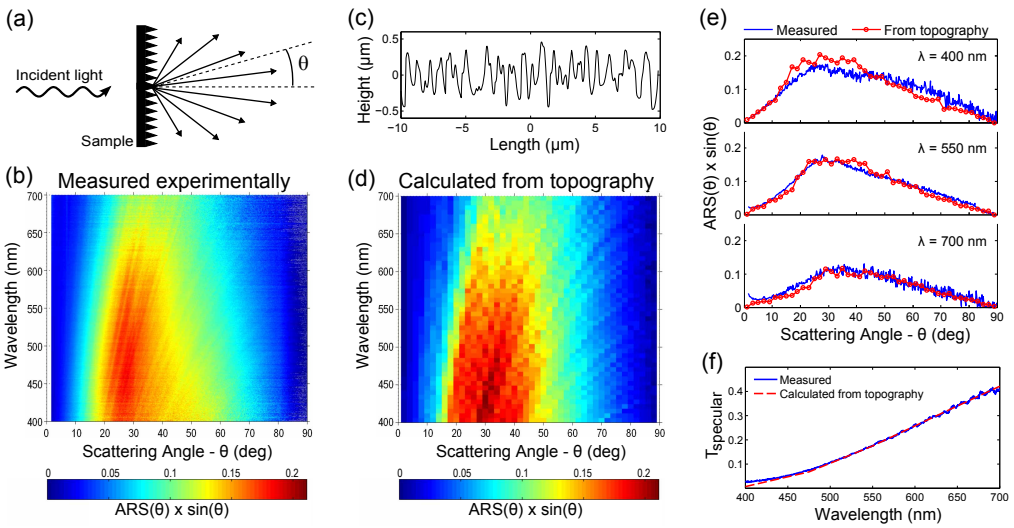

Fig. 3. (a) Sketch of the measurement geometry for angle resolved measurements. The data are collected with normal incident light and the detector is moved to various angles measuring the intensity as function of θ. (b) Measured angular resolved scattering ARS(θ) for visible wavelengths. The data are multiplied by a factor of $\sin\theta$ to achieve a probability distribution. (c) Typical profile from two dimensional scan recorded by AFM used for the modeling. (d) ARS(θ) calculated from a 20×20 μm^2 scan of the surface topography. The data are normalized to all propagating modes and multiplied by $\sin\theta$. (e) Comparison of the experimentally measured data and the data calculated from the surface topography for three different wavelengths. (f) Comparison of the measured specular transmittance and the specular transmittance calculated from the measured surface topography.

measurements of the angle resolved scattering (ARS) were performed on another sample with similar scattering characteristics as type 1 in Fig. 1(c). Under normal incident light, the transmitted intensity was measured as a function of scattering angle θ as illustrated in Fig. 3(a). The transmission haze $H_T = T_{\text{diff}}/T_{\text{total}}$ is the probability that an incoming photon is diffusely scattered [17]. The specular transmitted light T_{specular} and the transmission haze are related as $T_{\text{specular}} = 1 - H_T$. In Fig. 3(b), the intensity normalized to the intensity of the incoming light is plotted as function of wavelength and scattering angle. In order to convert the data to a probability distribution, they are multiplied by a factor of $\sin\theta$ and for each wavelength the data are normalized such that 2π times the integral over θ equals the transmission haze [17]. The light is most probable to be diffracted to an angle around 30 degrees and the shorter wavelengths are most likely to be scattered. This explains the orange color of the specular transmitted light.

ARS must be intimately connected to the surface topography. The measured ARS has been compared to predictions based on measurement of the surface topography and diffraction theory. The surface topography was measured by AFM and a typical profile from an AFM scan is seen in Fig. 3(c). The model is based on non-paraxial scalar diffraction theory [18, 19] and the used method is described in detail by Domine *et al.* [17].

While the overall qualitative agreement is seen by comparison of Fig. 3(b) and 3(d), the quantitative agreement can be evaluated in more detail in Fig. 3(e), where experimentally measured results and the results achieved from topographical information are compared directly for three different wavelengths. It is seen that the model predicts the scattering behavior of the surface structures very well.

It is also possible to make predictions for the specular transmittance using the surface to-

#161219 - $15.00 USD Received 10 Jan 2012; revised 2 Feb 2012; accepted 2 Feb 2012; published 7 Feb 2012

pography as the only input. In Fig. 3(f) the calculated and measured values of the specular transmittance are plotted as function of wavelength for the investigated surface. While a deviation is seen for wavelengths shorter than 500 nm, the model fits the measured data very well in the rest of the considered interval and the color appearance can be predicted from the AFM image.

The quality of the measured AFM data has proven to be important for the achieved result. The tips used were specially designed for high aspect ratio surfaces in order to be able to resolve relevant features of the surface. The same analysis has been carried out using a standard AFM tip. The result of this analysis showed an increase in the specular transmittance over the entire wavelength interval of up to 0.1 compared to the measured data shown in Fig. 3(f).

Although the AFM measurements have proven adequate for the topographical characterization of the investigated surface, it would be less straight forward to characterize surfaces with structures of higher aspect ratio in detail. This is for example the case for the surfaces of type 2 and type 3 in Fig. 1(b) because the shape of the AFM tip would influence the observed topography more significantly. For prediction of the transmittance for surfaces with such high aspect ratios one may have to investigate other techniques or thoroughly approximate the tip shape and correct for the influence on the observed topography.

4. Conclusion

In conclusion, a route to the realization of cheap single material color filters has been demonstrated based on the concept of light scattering on surface structures. Three distinct colors have been observed for three different surfaces. The scattering characteristics could be reproduced from topographical data and the specular transmittance spectrum could be predicted from a simple model which opens up new avenues for design of single-material plastic color filters.

Acknowledgments

The work was supported by the EC FP7 funded NaPANIL (Contract No. 214249) project and the NanoPlast project funded by the Danish National Advanced Technology Foundation (File No.: 007-2010-2). We thank professor Ole Sigmund for fruitful discussions, and acknowledge Emil Hoejlund-Nielsen and Thomas Buss for experimental assistance.

#161219 - $15.00 USD Received 10 Jan 2012; revised 2 Feb 2012; accepted 2 Feb 2012; published 7 Feb 2012